HHS Public Access

Author manuscript

Exp Eye Res. Author manuscript; available in PMC 2022 May 01.

Published in final edited form as:

Exp Eye Res. 2021 May ; 206: 108530. doi:10.1016/j.exer.2021.108530.

A smartphone based method for mouse fundus imaging

Michael Peng[a], **Bomina Park**[a,b], **Hemavathy Harikrishnan**[a], **Sultana N. Jahan**[a], **Jiannong Dai**[a], **Naga Pradeep Rayana**[a], **Chenna Kesavulu Sugali**[a], **Tasneem P. Sharma**[a,b], **Sanae Imanishi**[a], **Yoshikazu Imanishi**[a,b], **Timothy W. Corson**[a,b,c], **Weiming Mao**[a,c]

[a.]Eugene & Marilyn Glick Eye Institute, Department of Ophthalmology, Indiana University School of Medicine

[b.]Department of Pharmacology and Toxicology, Indiana University School of Medicine

[c.]Department of Biochemistry and Molecular Biology, Indiana University School of Medicine

Abstract

Noninvasive *in vivo* imaging of the mouse retina is essential for eye research. However, imaging the mouse fundus is challenging due to its small size and requires specialized equipment, maintenance, and training. These issues hinder the routine evaluation of the mouse retina. In this study, we developed a noncontact imaging system consisting of a smartphone, a 90D condensing lens, a homemade light diaphragm, a tripod, and a Bluetooth remote. With minimal training, examiners were able to capture fundus images from the mouse retina. We also found that fundus images captured using our system from wild type mice, mice with laser-induced retinal injury, and a mouse model of retinitis pigmentosa showed a quality similar to those captured using a commercial fundus camera. These images enabled us to identify normal structures and pathological changes in the mouse retina. Additionally, fluorescein angiography was possible with the smartphone system. We believe that the smartphone imaging system is low cost, simple, accessible, easy to operate, and suitable for the routine screening and examination of the mouse eye.

Keywords

Fundus imaging; Fluorescein angiography; Laser-induced retinal injury; Mouse retina; Retinitis pigmentosa; Smartphone

Fundus imaging is an essential diagnostic procedure in clinical ophthalmology. It allows the evaluation of pathological changes in the posterior segment of the eye including the optic nerve head, retinal vessels, and choroid. In particular, noninvasive *in vivo* imaging provides

Correspondence author: Weiming Mao Ph.D., Associate Professor, Eugene and Marilyn Glick Eye Institute, Department of Ophthalmology, Department of Biochemistry & Molecular Biology, Indiana University School of Medicine, RM305V, 1160 W. Michigan St, Indianapolis, IN, 46202, USA, weimmao@iu.edu, 1-317-278-0801.

the opportunity to longitudinally evaluate progressive changes in the disease processes of human patients.

To better understand ocular diseases, many mouse models have been developed to mimic human conditions. Therefore, there is a critical need to image the mouse fundus. In contrast to imaging the human fundus, imaging the mouse fundus faces additional difficulties because of its small size. The mouse eye is about 3mm in diameter (Park et al., 2012). So even when the mouse pupil is fully dilated, the area for light transmission is still limited, which requires a precise alignment of the imaging system. Further, since mice are not able to cooperate during eye examination, they have to be anesthetized and the entire imaging procedure relies solely on the operation and experience of the examiner.

A variety of mouse fundus imaging techniques have been described in the literature including using a high diopter condensing lens combined with a slit lamp biomicroscope, a surgical dissection microscope, or a fundus camera (Butler and Sullivan, 2015; DiLoreto et al., 1994; Hawes et al., 1999; Kocaoglu et al., 2007). Other commonly used methods include flattening the cornea using a coverslip or placing a contact lens on the cornea. Both methods aim to reduce the refractive power of the mouse cornea to facilitate fundus imaging (Cohan et al., 2003; Pinto and Enroth-Cugell, 2000). Some commercial devices such as the Micron IV system (Phoenix Research Laboratories, Pleasanton, CA) use a specialized objective which directly contacts the cornea to maximize light transmission. However, the commercially available mouse fundus imaging systems are costly. It is also inconvenient to use these systems for screening a large number of mice or in low-resource settings. Additionally, any imaging methods that require close corneal contact impose a risk of ocular infection.

An alternative approach for mouse fundus imaging is to use a smartphone and a condensing lens. This approach has already been used for human patients for several years, and has been proven to be very useful during emergencies or where there is a lack of ophthalmologic care (Lord et al., 2010). To image the human retina, a 20D biconvex aspherical condensing lens is placed in front of the eye after pupil dilation. The smartphone flashlight serves as a near coaxial light source, projecting light into the eye. Similar to a binocular indirect ophthalmoscope (BIO), the smartphone camera captures the light reflected back through the condensing lens, and forms an image on the screen. Since the smartphone camera has automatic focus and zoom functions, clear and magnified images can be obtained with minimal training compared to using a BIO. Additionally, this method requires no contact with the ocular surface, minimizing the risk of corneal injury or infection. Several groups have tried to apply the smartphone imaging approach to rodents. Mukai's group first reported the use of a smartphone and a 20D condensing lens to image the rabbit retina but the image quality was not ideal compared to that of the human retina (Haddock et al., 2013). The same group also reported in an ARVO abstract using a smartphone and a 78D condensing lens for mouse retinal fluorescein angiography (FA) (Qian et al., 2015). However, the authors did not show any bright-field fundus images. Here, we demonstrated that the smartphone paired with a 90D condensing lens can be used to produce high-quality bright-field images that are comparable to a commercial fundus imaging system such as the Micron IV and can also be used for FA.

To determine if our approach is suitable for mouse fundus imaging, we used an iPhone 6s (Apple, Cupertino, CA) plus a 90D condensing lens (Volk Optical, Mentor, OH). The iPhone camera and flashlight were controlled by a third-party application, Procam8 (https://www.procamapp.com/). To stabilize the smartphone, we mounted it on a tripod and imaging was controlled using a Bluetooth remote. We found that this setup was superior to holding the phone in one hand and tapping the phone's touch screen.

We compared 90D, 78D, and 60D condensing lenses (data not shown), and found that the 90D lens provided the best image quality and a wider angle of view for the mouse fundus. To reduce interference from light reflected from outside the mouse fundus, we used a custom-made diaphragm (Figure 1). The 90D condensing lens was inserted into one end of a rubber gasket removed from a ¾ inch Sch40 PVC compression coupling. A 3.5 cm long PVC pipe (3/4 in, Sch 40) was cut, and the inside was spray-painted with a flat black oil-based paint to reduce stray light reflection while the outside was wrapped with black electrical tape to enhance grip. The diaphragm was constructed such that the edge of the lens was flush with the end of the gasket and the PVC pipe was seated directly behind the lens to secure it in place (Figure 1B and 1C).

To test the smartphone's ability to distinguish normal and pathological mouse retinas, three mouse models were used in this study: 8 week old wild type (WT) C57BL/6J male mice (Jackson laboratory, Bar Harbor ME), 8 week old C57BL/6J male mice with laser-induced retinal injury, and a retinitis pigmentosa (RP) mouse model on a C57BL/6J background (8 month old, male). The mice were housed at the Indiana University School of Medicine animal facility and all experiments were approved by the Institutional Animal Care and Use Committee. To induce retinal injury under anesthesia, four laser burns per eye were made around the optic nerve head using an argon green ophthalmic laser at 50 μm spot size, 70 ms, and 250 mW pulses, and the procedure was monitored using the Micron IV system (Phoenix Research Laboratories) (Merrigan et al., 2020). Mice were imaged immediately after laser treatment. To study retinal degeneration, a retinitis pigmentosa (RP) mouse model exhibiting photoreceptor degeneration was used. These mice harbored a class I rhodopsin mutation, which changed glutamine at position 344 to a stop codon (Q344*). The same mutation was found in human patients with autosomal dominant retinitis pigmentosa (Sung et al., 1991).

For Micron IV imaging, the mice were anesthetized by intraperitoneal injection of 90 mg/kg ketamine hydrochloride and 5 mg/kg xylazine mixture. The anesthetized mouse was placed on a multi-axis positioner. The eyes were lubricated with 2.5 % Gonak hypromellose ophthalmic solution (Akorn Inc., Lake Forest, IL) and brought into contact with the camera objective. After adjusting focus and brightness, bright-field live fundus imaging was performed using the manufacturer's image acquisition software.

For smartphone imaging, the mice were anesthetized using isoflurane (2.5%; inhalation) or intraperitoneal injection of 90 mg/kg ketamine hydrochloride and 5 mg/kg xylazine mixture if Micron IV imaging was conducted at the same time. When both imaging systems were used for the same mouse, smartphone imaging was done before Micron IV imaging because Gonak was difficult to remove from the mouse eye. The anesthetized mice were given

topical 1% tropicamide (Henry Schein Inc., Melville, NY) followed by 2.5% phenylephrine hydrochloride (Paragon BioTeck Inc., Portland, OR) for pupil dilation. Both eyes were periodically hydrated with PBS to prevent corneal drying and clouding which could compromise light transmission and image quality.

Materials and setup of the smartphone imaging system are shown in Figure 1. The anesthetized mouse was placed on a heating pad on a raised platform. The smartphone was mounted on a tripod, about 14 cm from the mouse eye, and the camera and flashlight were pointed and focused on the mouse cornea. Through the Procam8 application, the digital image was zoomed in to 5x and the phone flashlight was turned on. We found that the initial positioning of the tripod to align the camera with the visual axis was the key to successful imaging. During this process, fine adjustments were made to keep the red fundus reflex visible. Once alignment was achieved, the same setting could be applied to the other mice to be examined/imaged with little adjustment. The examiner held the 90D condensing lens in one hand, and carefully positioned it between the smartphone camera and mouse eye. We found that it was helpful to gradually move the condensing lens from the smartphone camera towards the mouse eye while keeping the red reflex centered until a fundus image appeared on the smartphone screen. A clear image was formed when the condensing lens was positioned about 1cm in front of the mouse eye. There was no contact between the eye and condensing lens. Both automatic and manual focus as well as exposure settings could be adjusted using the other hand. Notably, the peripheral retina or another region of interest could be imaged by carefully manipulating the mouse/platform and the condensing lens without having to adjust the tripod and smartphone. Once the desired image was displayed on the smartphone screen, images were quickly acquired via the burst function (capture of a series of images) and stored in the smartphone.

For FA, WT mice were anesthetized and pupils were dilated as above. One percent fluorescein was administered by intraperitoneal injection at 10 μl/g body weight. Five to ten minutes post-injection, FA was performed using the Micron IV system with spectral band filters optimal for fluorescein: an excitation filter (FF01–469nm/35nm, Semrock, Rochester, NY) and a barrier filter (BLP01–488nm long pass edge filter, Semrock). Smartphone FA imaging was performed using the same mouse eyes on a different day in order to compare the images at a similar phase (5–10 minutes post-injection). The excitation and barrier filters from the Micron system were removed and taped to the flashlight and camera of the smartphone, respectively, for smartphone FA imaging.

All the materials and their costs are listed below:

1. Smartphone: iPhone 6S (Apple); already available, cost not included.
2. Tripod and Bluetooth remote: UBeesize Tripod S, Premium Flexible Phone Tripod with Wireless Remote Mini Tripod Stand for Camera GoPro/Mobile, Amazon, Seattle, Washington; $19.99.
3. Procam8 application: Apple App Store; $6.99.
4. 90D condensing lens: Volk 90D, Volk, $380.

5. Sch40 3/4in PVC pipe: Catalog #: PVC040070200, The Home Depot, Atlanta, GA; $1.35.
6. Sch40 3/4 inch compression coupling (for the rubber gasket): Catalog #: 511–43-34–34H, The Home Depot, Atlanta, GA; $5.10.
7. Spray paint: Rust-Oleum Painter's Touch 2X, Catalog #: 334020, The Home Depot, Atlanta, GA; $3.98.
8. Excitation and barrier filters: removed from the Micron Imaging System; already available, cost not included.

Using our smartphone imaging setup, we obtained high-quality bright-field images of the mouse fundus. Representative bright-field images taken from our smartphone imaging system (Figure 2A, 2C and 2E) and from the Micron IV system (Figure 2B, 2D and 2F) were compared. For each mouse model, the same eye was imaged using both imaging systems. The optic nerve head and retinal blood vessels were clearly visible in both systems. The overlying vessels from the retina as well as the radial pattern of retinal ganglion cell nerve fibers (especially in Figure 2E) appeared to be more distinguishable with the smartphone system. Both systems showed the pathological changes of laser-induced retina burns and a small retinal hemorrhage (Figure 2C and 2D) as well as those of the retina of the RP model mouse, including a waxy-colored optic nerve head and attenuation of retinal blood vessels (Figure 2E and 2F) compared to WT controls (Figure 2A and 2B). These vascular changes are consistent with previous studies of RP mouse models that indicated vascular narrowing in the retina (Hawes et al., 1999). Hawes et al. also indicated hypo- and hyper-pigmentation of RPE in RP mouse models (Hawes et al., 1999). Although no mottled pattern of RPE was detected, we noticed the fundus color of the RP model mouse was different from that of the WT mouse, which was probably due to changes in RPE pigmentation or loss of photoreceptors affecting light transmission and reflection.

Although the 90D condensing lens is aspherical, there may still be spherical aberration. To compare spherical aberration between the smartphone and Micron IV systems, we compared the ratio of the diameter of the centrally located optic disc vs. the diameter of one of the peripherally located laser burns (Figures 2C and 2D, black lines). A higher ratio represents higher spherical aberration in the imaging system.

$$\frac{d_2}{d_1} vs \cdot \frac{D_2}{D_1}$$

The diameters (the black lines in Figure 2C and 2D) were measured using Image J (National Institute of Health, Bethesda, MD) in arbitrary units:

Smartphone system= 0.43/0.25 = 1.72

Micron IV system= 0.46/0.28= 1.64

The calculated ratios were very close, suggesting the levels of spherical aberration between the two systems are almost the same. Additionally, we found that the field of view of the

smartphone imaging system was similar to that of the Micron IV system (50 degrees according to manufacturer's specification).

We also obtained FA images of the mouse fundus using the same filters as those in the Micron IV system (Figure 2G and 2H). In contrast to bright-field images, the resolution of FA images was lower than that of Micron IV images. Although the 12 major retinal blood vessels that were clearly visible in the Micron IV system were also detected by the smartphone system, the signal intensity in the latter system was much lower (Figure 2G vs. 2H, numbers 1–12). Also, two small branches were not visible in the smartphone system (Figure 2G vs. 2H, numbers 13–14). The low resolution and low signal-to-noise ratio of the smartphone FA image were likely due to the low power of the excitation light source (the flashlight of the smartphone vs. the Xenon arc lamp in the Micron IV system) and camera sensitivity. The smartphone had to be set at high ISO setting which was equivalent to binning (combining pixels) to increase sensitivity for FA signal.

Overall, image acquisition using the smartphone system can be accomplished by a single operator. The initial setup took less than 10 minutes, and imaging the fundus took about 1 minute per eye when operated by experienced users. Additionally, three of our lab members with no prior experience of using a BIO or condensing lens were able to obtain fundus images within 5–15 minutes during their first training. The most difficult part for a novice was to manipulate the 90D condensing lens due to the inverted image display. However, we found that it only required minimal practice to become accustomed to the technique.

There are several advantages of the smartphone imaging system compared to commercial systems:

1. Low cost, simplicity and portability. The smartphone system requires only a condensing lens and a smartphone. In contrast, the commercial system requires designated space and its transportation needs special caution. The use of both systems requires training, but based on our experience, the amount of training needed for the smartphone system was equivalent to the Micron IV system. The total cost excluding the smartphone and filters was approximately $420. The total cost could have been much lower if the 90D condensing lens (~90% of total cost) was already available or borrowed from the clinic.
2. The use of inhalation anesthetics. Using the smartphone imaging system, mice can be placed on a variety of platforms for inhalation anesthesia e.g. isoflurane. In contrast, it is difficult to mount the induction tube and nose adaptor for inhalation anesthetics to the Micron IV system. Using inhalation anesthesia provides an additional advantage of minimizing lens opacity or corneal damage since both of which were reported in mice anesthetized using ketamine/xylazine (Calderone et al., 1986; Staff, 2015).
3. Decreased risk of ocular infection and contamination. Unlike the commercial system or using a coverslip to flatten the cornea, the smartphone imaging system has no direct corneal contact and therefore minimizes the risk of ocular infection, abrasion, and contamination. This advantage could also be used to visualize

procedures such as intravitreal injection in real time. However, it would require two people, one for injection and one for imaging.

4. Fundus color. We previously examined the mouse fundus using a 90D condensing lens and a BIO. Our experience was that the color of the smartphone image was closer to what we observed using a BIO. In contrast, the hue of the fundus image generated by the Micron IV was more “red” as seen in Figure 2.

However, we also noticed several limitations of the smartphone imaging system:

1. Retinal vessel shadows, glare/light reflection, and chromatic aberration. At certain angles, retinal vessel shadows were visible (Figure 2A, triangles). This was likely due to the uneven illumination of the fundus by the light source of the smartphone. Since the flashlight beam is not perfectly co-axial to the camera light pathway, the light beam projected onto the retina may create shadows of the vessels. Similar shadows were not observed in the Micron IV system. Also, glare/light reflection and chromatic aberration were observed which might partially obstruct the view of the smartphone system (Figure 2A, 2C, and 2E, arrows). We found that glare could be avoided by tilting the 90D condensing lens. However, tilting the 90D condensing lens did not eliminate shadows or chromatic aberration.

   We also tested another approach: the smartphone was attached to a phone case on which a long PVC pipe, the rubber gasket, and the 90D condensing lens were also fixed. Although this approach made it easier to locate and image the mouse fundus since there was little adjustment needed, it was impossible to tilt the condensing lens. The only way to reduce shadows or to avoid light reflection using that approach was to adjust the mouse position. We found that adjusting the mouse was more difficult and time-consuming than manipulating the 90D condensing lens by hand. Therefore, we decided to use the current system with the lens separated from the smartphone.

2. Consistency. While high quality images can be obtained after training, there are technical variabilities among users. This is because the smartphone imaging system has more adjustable parameters, such as the distance from the condensing lens to the mouse, the distance from the condensing lens to the camera, and 90D condensing lens angle. In contrast, the Micron IV system requires the adjustment of only the distance between the lens and mouse eye.

3. Resolution. The resolution of the fundus image for bright-field imaging was equivalent to the Micron IV system. However, it is much lower than a confocal scanning laser ophthalmoscope, which is able to distinguish the detail within the nerve fiber layer or microvasculature of the retina (Paques et al., 2006). Additionally, the Micron IV system showed much better resolution and signal intensity for FA compared to the smartphone system.

4. Lack of other applications. A commercial system like the Micron IV usually combines a fundus camera, FA module, OCT module, laser module, ERG module, and anterior segment imaging module in one unit or as optional

attachments. In contrast, the smartphone system can currently only be used for bright-field imaging and FA. However, its low cost somewhat mitigates its limitation.

In summary, we describe a smartphone and 90D condensing lens based approach for mouse fundus imaging. We found that this approach generated comparable results to the Micron IV imaging system using the three mouse models described. This technique is simple, easy to operate, and suitable for mouse fundus screening, examination, and documentation. We expect that with the advancement of smartphone technologies, especially photosensors, light sources, and imaging software, fundus image quality will be further improved.

Acknowledgements

This study was supported by NEI R01EY026962 (WM), R01EY025641 (TWC), R01EY031939 (TWC), Indiana University School of Medicine Showalter Scholarship (WM), BrightFocus Foundation G2017151 (WM), and the Indiana Clinical and Translational Sciences Institute funded, in part by Award Number UL1TR002529 from the National Institutes of Health, National Center for Advancing Translational Sciences, Clinical and Translational Sciences Award (WM). The content is solely the responsibility of the authors and does not necessarily represent the official views of the National Institutes of Health.

Abbreviations

BIO	binocular indirect ophthalmoscope
LRI	laser-induced retinal injury
RP	retinitis pigmentosa
WT	wild type

References

Butler MC, Sullivan JM, 2015. A Novel, Real-Time, In Vivo Mouse Retinal Imaging System. Invest Ophthalmol Vis Sci 56, 7159–7168. [PubMed: 26551329]

Calderone L, Grimes P, Shalev M, 1986. Acute reversible cataract induced by xylazine and by ketamine-xylazine anesthesia in rats and mice. Exp Eye Res 42, 331–337. [PubMed: 3754819]

Cohan BE, Pearch AC, Jokelainen PT, Bohr DF, 2003. Optic disc imaging in conscious rats and mice. Invest Ophthalmol Vis Sci 44, 160–163. [PubMed: 12506069]

DiLoreto D Jr., Grover DA, del Cerro C, del Cerro M, 1994. A new procedure for fundus photography and fluorescein angiography in small laboratory animal eyes. Curr Eye Res 13, 157–161. [PubMed: 8194363]

Haddock LJ, Kim DY, Mukai S, 2013. Simple, inexpensive technique for high-quality smartphone fundus photography in human and animal eyes. J Ophthalmol 2013, 518479. [PubMed: 24171108]

Hawes NL, Smith RS, Chang B, Davisson M, Heckenlively JR, John SW, 1999. Mouse fundus photography and angiography: a catalogue of normal and mutant phenotypes. Mol Vis 5, 22. [PubMed: 10493779]

Kocaoglu OP, Uhlhorn SR, Hernandez E, Juarez RA, Will R, Parel JM, Manns F, 2007. Simultaneous fundus imaging and optical coherence tomography of the mouse retina. Invest Ophthalmol Vis Sci 48, 1283–1289. [PubMed: 17325174]

Lord RK, Shah VA, San Filippo AN, Krishna R, 2010. Novel uses of smartphones in ophthalmology. Ophthalmology 117, 1274–1274 e1273. [PubMed: 20522335]

Merrigan SL, Park B, Ali Z, Jensen LD, Corson TW, Kennedy BN, 2020. Calcitriol and non-calcemic vitamin D analogue, 22-oxacalcitriol, attenuate developmental and pathological choroidal vasculature angiogenesis ex vivo and in vivo. Oncotarget 11, 493–509. [PubMed: 32082484]

Paques M, Simonutti M, Roux MJ, Picaud S, Levavasseur E, Bellman C, Sahel JA, 2006. High resolution fundus imaging by confocal scanning laser ophthalmoscopy in the mouse. Vision Res 46, 1336–1345. [PubMed: 16289196]

Park H, Qazi Y, Tan C, Jabbar SB, Cao Y, Schmid G, Pardue MT, 2012. Assessment of axial length measurements in mouse eyes. Optom Vis Sci 89, 296–303. [PubMed: 22246334]

Pinto LH, Enroth-Cugell C, 2000. Tests of the mouse visual system. Mamm Genome 11, 531–536. [PubMed: 10886018]

Qian C, Hasegawa E, Haddock L, Wu D, Mukai S, 2015. Smartphone fundus photography, in vivo retinal fluorescent photography and fluorescein angiography in mouse eyes [Abstract]. IOVS 56.

Staff, P.O., 2015. Correction: Ketamine/Xylazine-Induced Corneal Damage in Mice. PLoS One 10, e0137559. [PubMed: 26327227]

Sung CH, Davenport CM, Hennessey JC, Maumenee IH, Jacobson SG, Heckenlively JR, Nowakowski R, Fishman G, Gouras P, Nathans J, 1991. Rhodopsin mutations in autosomal dominant retinitis pigmentosa. Proc Natl Acad Sci U S A 88, 6481–6485. [PubMed: 1862076]

Highlights

- A technique for imaging the mouse fundus using a smartphone and 90D condensing lens.
- Bright-field image quality was comparable to a commercial mouse retinal imaging system.
- Both normal fundus and pathological changes in the fundus could be differentiated.

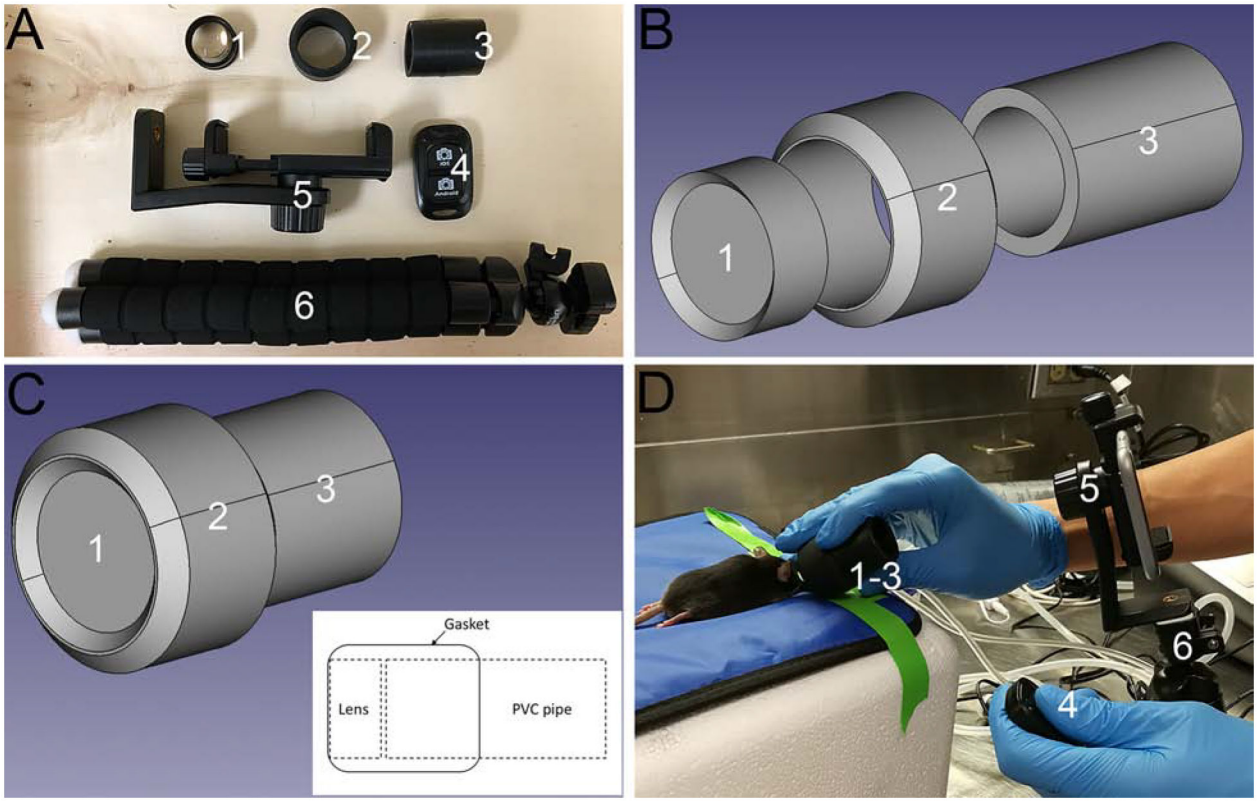

Figure 1:

Materials and setup of the smartphone imaging system.

(A) Individual components of the smartphone imaging system. 1: 90D condensing lens; 2: ¾ inch Sch40 PVC compression coupling rubber gasket; 3: 3.5 cm long ¾ inch PVC pipe with black spray paint inside and black electrical tape outside; 4: Bluetooth remote; 5: adjustable smartphone holder; 6: tripod. (B) and (C): assembly of the diaphragm using the 90D condensing lens (1), rubber gasket (2), and PVC pipe (3). The 90D condensing lens and PVC pipe were inserted into the rubber gasket with the lens flush with the front of the gasket and the PVC pipe seated directly behind the lens within the gasket. (D) Smartphone imaging system setup. The assembled diaphragm (1–3) was positioned between the mouse eye and smartphone mounted on the holder (5) and tripod (6) until the fundus image was shown on the smartphone screen. Fundus images were captured via the Bluetooth remote (4).

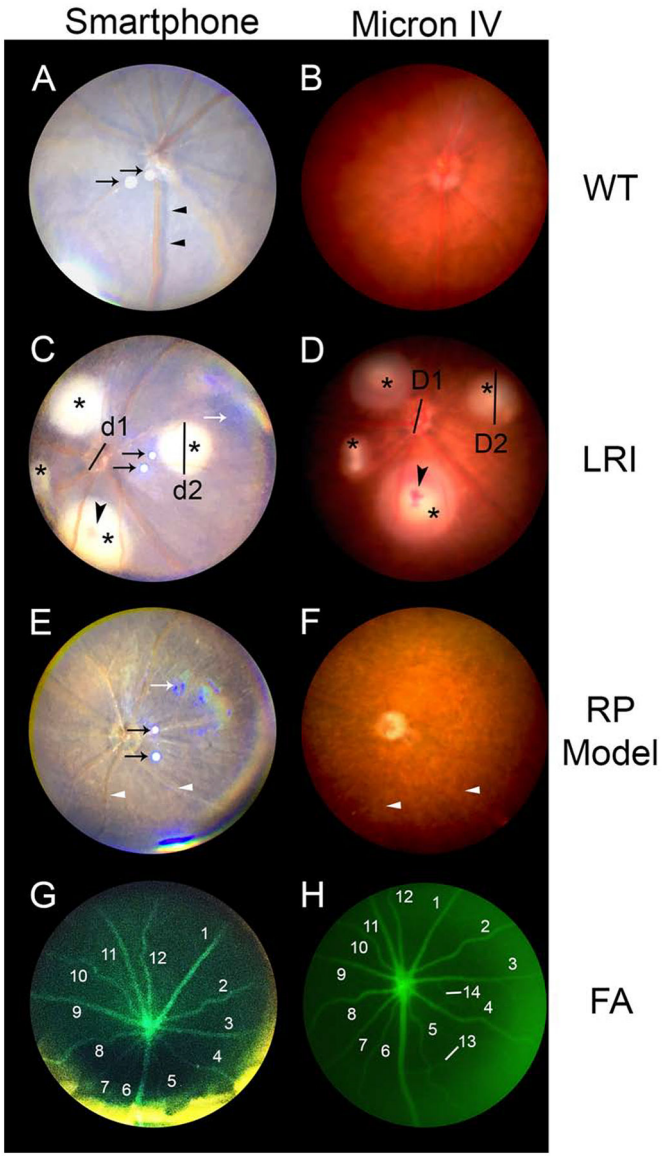

Figure 2:

A comparison of fundus images obtained using the smartphone and Micron IV imaging systems. Each pair of images were taken from the same mouse eye. For image comparison, the entire visible fundus area was cropped, stretched, and presented at the same image size for the two systems. (A) and (B): wild-type (WT) C57BL/6J mouse retina. (C) and (D): laser-induced retinal injury mouse retina (LRI). (E) and (F): retinitis pigmentosa (RP) model mouse retina. (G) and (H): fluorescein angiography (FA) of WT retina. Black arrows: glare/light reflection. White arrows: chromatic aberration. Black triangles: retinal vessel shadow. White triangles: attenuated retinal blood vessels. Asterisks: laser burns. Arrowheads: hemorrhage. The black lines in (C) and (D): diameters of the optic disc (d1 or D1) and diameters of the laser burn (d2 or D2), respectively. The numbers in (G) and (H): retinal blood vessels.